Water organization between oppositely charged surfaces: Implications for protein sliding along DNA[a)]

Amir Marcovitz, Aviv Naftaly, and Yaakov Levy[b)]
Department of Structural Biology, Weizmann Institute of Science, Rehovot 76100, Israel

(Received 11 September 2014; accepted 5 February 2015; published online 27 February 2015)

Water molecules are abundant in protein–DNA interfaces, especially in their nonspecific complexes. In this study, we investigated the organization and energetics of the interfacial water by simplifying the geometries of the proteins and the DNA to represent them as two equally and oppositely charged planar surfaces immersed in water. We found that the potential of mean force for bringing the two parallel surfaces into close proximity comprises energetic barriers whose properties strongly depend on the charge density of the surfaces. We demonstrated how the organization of the water molecules into discretized layers and the corresponding energetic barriers to dehydration can be modulated by the charge density on the surfaces, salt, and the structure of the surfaces. The 1–2 layers of ordered water are tightly bound to the charged surfaces representing the nonspecific protein–DNA complex. This suggests that water might mediate one-dimensional diffusion of proteins along DNA (sliding) by screening attractive electrostatic interactions between the positively charged molecular surface on the protein and the negatively charged DNA backbone and, in doing so, reduce intermolecular friction in a manner that smoothens the energetic landscape for sliding, and facilitates the 1D diffusion of the protein. © *2015 AIP Publishing LLC.* [http://dx.doi.org/10.1063/1.4913370]

INTRODUCTION

Water molecules play a key role in many biological functions. They are abundant in many protein–protein and protein–DNA interfaces[1–4] and are known to associate with the native structure of many regulatory proteins and enzymes that bind DNA specifically.[5–8] Although interfacial solvent molecules exchange rapidly with the bulk solvent, structural and biochemical data suggest that the presence of water in protein–DNA interfaces is essential and that water molecules are major constituents of specific protein–DNA complexes.[9–11] However, both experimental and theoretical studies on the thermodynamics of protein–DNA binding support the view that the displacement of ordered water molecules from the interface is entropically favorable, thus contributing to the stability of the complex.[12–14] Remaining solvent at the interface plays an important structural role in the stability and specificity of protein–DNA interfaces as water molecules may mediate hydrogen bonds between the protein and DNA, screen unfavorable electrostatic interactions, and may serve as "fillers" of unoccupied spaces in the complex.[9,15] A role for small ions as regulators of specificity in protein–DNA recognition was also proposed,[16] and suggests that some of the counterions that condense on DNA are displaced upon specific protein–DNA binding, which further contributes to binding by increasing its entropic favorability. Structural studies showing clusters of solvent molecules at the interface of nonspecific protein–DNA complexes[17,18] and the notion that sequence-specific DNA binding is dominated by dehydration[12,14] suggest that an important distinction between specific and non-specific protein–DNA complexes is the number of ordered water molecules at the interface.

An efficient search mechanism undertaken by a DNA-binding protein for a specific DNA target will require that the non-specifically bound protein avoid over-sampling each base-pair in the DNA grooves during sliding (i.e., one-dimensional diffusion of the protein that is characterized by a rotation-coupled translation dynamics by following the DNA major groove), and that the ruggedness of the landscape for traversal sliding will remain in the order of ~1–2 k_bT.[19,20] This requirement is achieved, at least partially, by relying on electrostatic (i.e., nonspecific) interactions between the searching protein and the DNA.[21] Weak electrostatic interactions allow the proteins to slide along the non-specific DNA, and in some cases, two distinct conformations are required to minimize possible formation of hydrogen bonds between the proteins and the DNA that may slow down sliding by trapping the protein.[22,23] It was also shown that the strength of the electrostatic patch on the DNA-binding protein may affect the speed of its sliding diffusion.

While several studies have recently investigated how the molecular properties of the proteins and of the DNA affect sliding,[24–27] it is still unclear how water and ions mediate the search process. This raises the question of whether the relatively hydrated interface of the nonspecific protein–DNA complex plays a role in assisting protein sliding along DNA by reducing intermolecular friction at the protein–DNA interface and, if so, in what way this solvent-assisted sliding is affected by the electrostatic properties of the interacting molecular surfaces. Using computer simulations and analytical calculations based on a simplified non-specific protein–DNA model,

[a)]This article is part of the Special Topic on Biological Water.
[b)]Author to whom correspondence should be addressed. Electronic mail: koby.levy@weizmann.ac.il

Dahirel *et al.*[28] demonstrated that repulsion between the two biomolecules exists at very small separations. A barrier, therefore, separates the hydrated state from the dehydrated state and allows the protein to easily slide along the DNA when it is in the hydrated state.[28] The source for this repulsive force is suggested to be ions dissolved in the solution that condense on the densely negatively charged DNA. As the protein approaches the surface of the DNA, ions become trapped in the narrowing interfacial gap, creating a local region of high salt concentration. Water molecules try to move into this region, and the resulting osmotic pressure pushes out on the protein. This mechanism, which depends on the charge asymmetry of the two interacting molecules, was shown to be affected by the magnitude of the charge densities of the molecules as well as by their geometrical complementarity.

In this article, we study a model of two oppositely charged surfaces immersed in water in the absence and presence of salt to study the atomistic details of the mechanism by which water may facilitate protein sliding along DNA. The forces between oppositely charged surfaces were investigated in the past in several insightful studies.[29–31] Our study aims at providing microscopic understanding of the interactions between charged surfaces, the resulting repulsion between them, and the organization of the water molecules in the protein–DNA biomolecular interface. We calculated the potential of mean force (PMF) for bringing the two parallel plates of opposite charges into close proximity, and observed repulsive free energy barriers at short range and additional smaller barriers along the pathway resulting from the removal of ordered solvent layers. These observations imply that the solvent and ions play a crucial role in mediating nonspecific protein–DNA interactions *in vivo*.

METHODS

The studied systems were composed of two oppositely charged parallel plates, to represent the DNA and protein halves of the interaction, that were solvated in an aqueous solution in the absence or presence of salt. We employed a solvated plate–plate system model that was previously used to study the effect of denaturants on hydrophobic molecular surfaces.[32] Each plate comprised a 6×6 lattice of bonded carbon-like spherical atoms modeled using the AMBER molecular dynamics (MD) simulation software package. AMBER atoms of type carbon were used for the carbon-like dummy plate atoms, and the van der Waals parameters for interaction with water oxygen atoms were set to (σ) of 0.34 nm and $\varepsilon = 0.036$ KJ/mol, so creating a surface of 2.25 nm^2 (i.e., 3 Å lattice spacing) as exemplified in the inset of Figure 1. To test the effect of the size of the surface, we also studied larger surfaces comprised of 9×9 and 12×12 beads. Varying amounts of negative charge were assigned to each of the negative plate spheres in each system, such that the overall surface charge density, σ^-, was equivalent to that of *B*-DNA. We assigned positive charges to the spheres of the positively charged surface to obtain different systems with several σ^+ values. The charges of the surfaces were assigned to achieve charge densities ranging between 1 and 10 e nm^{-2}. To examine the effect of salt on the interaction between the two plates, the systems were studied

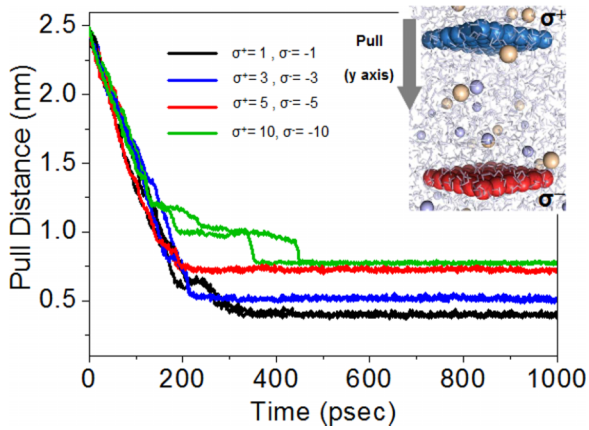

FIG. 1. Constant force pulling trajectories for a positively charged plate (blue surface) approaching a negatively charged plate (red surface). Pulling is performed in the solvent along the y-axis. At higher surface charge densities (for example, $\sigma^+ = 10$ e nm^{-2} pulled to $\sigma^- = -10$ e nm^{-2}, green line), the pulling path becomes discontinuous, and the positive surface becomes trapped at specific distances along the pathway. The pink and blue spheres correspond to chloride and sodium ions, respectively.

also in the presence of several ions (NaCl, KCl, and $MgCl_2$) at a concentration of 0.5 M. We also studied the behavior of water next to charged plates composed of smaller and larger beads (diameters of 2 and 4 Å, respectively).

The systems were studied with MD simulations at an atomistic resolution using the GROMACS-4.0.7 software package[33] with the AMBER99 force field,[34] particle mesh Ewald electrostatics (pme_order = 4, fourierspacing = 0.16), a Nośe-Hoover thermostat, and a Parinello-Rahman barostat ($\tau_p = 2$ ps, p = 1 bar). We started by solvating the plates in a periodic boundary box (with dimensions of $4.5 \times 6.5 \times 4.5$ nm) using the TIP3P water model and ions at a concentration of 0.5 M. Plate atoms were restrained to their positions, and the solvent and ions were energy minimized, followed by a short NVT (constant volume-temperature) equilibration at 300 K, and NPT (constant pressure-temperature) equilibration to a pressure of 1 bar. The system was then simulated for an additional 10 ns to allow full equilibration of the ions and solvent with the plates.

The PMF for each system was generated with the umbrella sampling technique in two steps. First, the positively charged surface, initially positioned at a distance (along the y-axis) of 2.5 nm from the negatively charged surface, was pulled for 3 ns at a constant force toward the negative surface (Figure 1, arrow) which was restrained to its position. During this pulling phase, we obtained 75–80 equally spaced frames along the pathway. In the second step, we performed 20 ns umbrella simulations where a harmonic potential with a force constant of 2×10^4 kJ mol^{-1} nm^{-2} was applied between the centers of mass of the two plates, using the previously collected frames as input configurations for each such run. From the resulting trajectories, we extracted the PMF of the two surfaces as they approached each other using the weighted histogram analysis method (WHAM).[35] The umbrella sampling simulations were used to analyze the organization of the water molecules next to the charged surfaces. In addition to the umbrella sampling simulations, pulling simulations were performed at mild forces (100 and

500 kJ mol^{-1} nm^{-2}) to pull the positive surface toward the negative surface in order to probe the kinetics of the dehydration of the charged surfaces.

RESULTS

Oppositely charged surfaces in solution repel each other at short ranges

To simplify nonspecific protein–DNA associations, we used atomistic MD simulations to calculate the free energy landscape for bringing two surfaces that bear opposite charge densities (σ^+, σ^-) into close proximity in solution. Figure 1 demonstrates a pulling trajectory of the positive surface (analogous to a DNA-binding protein surface) toward the fixed negative surface (analogous to a DNA sugar-phosphate backbone) using a force constant of 500 kJ mol^{-1} nm^{-2}.[33] In the early stages of pulling, when the separation distance between the surfaces is greater than ~1.2 nm, the pulling procedure is uniform and has no dependence on the electrostatic properties of the plates. However, as the two surfaces approach each other to within ranges of ~0.4–1.1 nm, the pulling procedure encounters barriers that become more significant as the charge densities on the plates increase (see Figure 1 for pulling of a positive plate towards a negative plate bearing a surface charge density of the same magnitude for $|\sigma|$ = 1, 3, 5, or 10 e nm^{-2}). When the charge densities on the plates increase, the system is trapped at larger separation distances between the two plates, which create a step-like feature in the pulling trajectory. The trapping of the two oppositely charged plates at larger distances and the apparent high free energy barrier for their dehydration might be related to both water–water and water–surface interactions.

To capture the energetics of bringing the two oppositely charged surfaces into contact, we calculated the PMF for the association of surfaces of different charge densities (Figure 2). In addition, we calculated the PMF for bringing two uncharged plates (σ = 0) together and found a significantly favorable free energy gain, most probably resulting from a depletion force (i.e., an entropic gain from releasing the water at the interface between the two surfaces into the bulk upon their association). We note that the free energy change upon association of the two neutral plates depends linearly on the size of the surfaces. The PMF for bringing two neutral plates together is downhill (i.e., barrierless) independently of the size of the plates, but the energetic gain upon association is larger for larger plates (the free energy gain upon association of 3×3, 6×6, 9×9, and 12×12 plates is 10, 20, 50, and 80 kcal/mol, respectively).

Apparently, an increase in the surface charge densities on the plates (from σ = 0 up to $|\sigma|$ = 10 e nm^{-2}) induces energetic barriers that appear at plate–plate separation distances of less than 10 Å. When located in a low-energy trap (Figure 2(a)), the positively charged plate remains at a certain distance from the negatively charged plate. The association of the surfaces is dominated by a single barrier for σ = 1 e nm^{-2}. When the charge density is increased to 3 e nm^{-2}, another barrier is added to the PMF. Not only do the barriers become higher as the charge density on the surface increases but also the number of barriers increases too. The

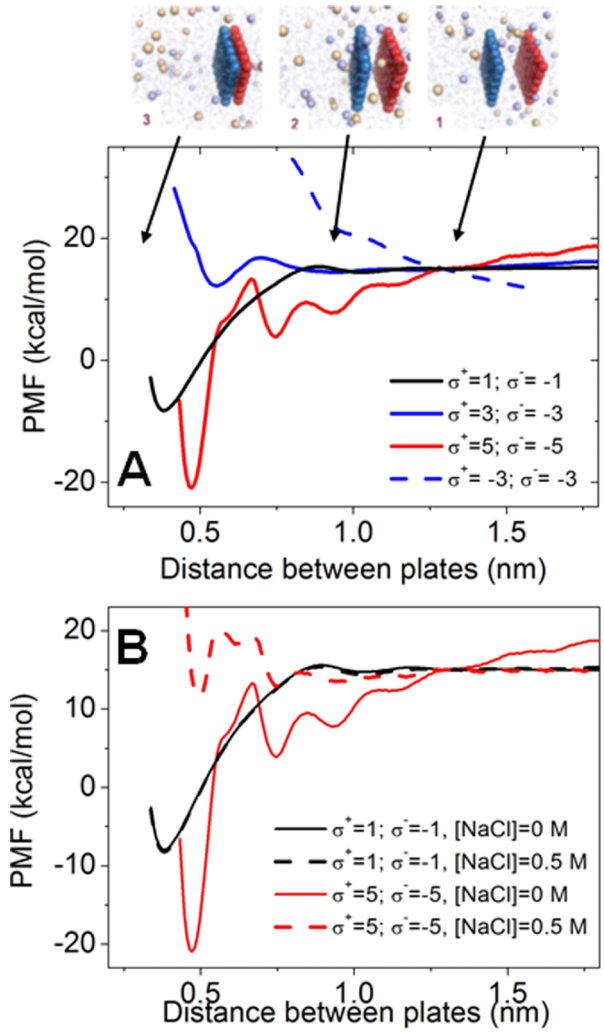

FIG. 2. PMF describing the process of bringing two charged plates (blue, positively charged; red, negatively charged) into contact with each other. (a) PMF for association of oppositely charged surfaces in water. Larger surface charge densities ($|\sigma|$ = 5 e nm^{-2}, red line) impose free-energy barriers on the order of ~5–10 kcal mol^{-1} along the pathway (i.e., at plate separation distances of ~0.6–1.2 nm), in agreement with the pulling trajectories (Fig. 1). The profile for bringing two negatively charged plates together (immersed in a neutralized simulation cell) shows a sharp increase in free energy due to water polarization. The snapshots illustrate the system state as interfacial solvent is removed along the path. The dashed line represents the PMF between two surfaces of like charge magnitude ($\sigma^- = \sigma^+ = |3|$). (b) PMF for association of oppositely charged surfaces in the absence and presence of salt.

PMF for the plate with σ^+ = 5 e nm^{-2} includes several additional barriers. This suggests that the water molecules are more organized next to surfaces with higher charge densities and such surfaces exert a longer range effect.

The magnitude of the barrier decreases when salt is added, which suggests that salt affects the structure of the hydration layers. This is seen for surfaces with σ = 3, however, for surfaces with σ = 1, the addition of salt does not affect the interactions between the plates because the interactions between the ions and the plates are weak (Figure 2(b)). In most of the PMF plots, it was not possible to sample the complete dehydration of the interface between the two plates (i.e., direct interactions between the positive and negative surfaces), presumably because of the very high barrier that needs to be overcome. We propose that the ruggedness of the

free energy landscape at separation distances of 0.5-1.0 nm will prevent partial dehydration (i.e., the removal of the 1st layer of water molecules, see Fig. 4 (left)) in realistic molecular systems. Complete dehydration of the plate interfaces (i.e., removal of the first layer of water molecules) is achieved for inter-distance below 0.3 nm (for highly charged plates, the free energy barrier for complete dehydration could not be satisfactorily sampled, but this barrier is so high that complete dehydration is irrelevant, even in specific complexes). Specifically, in protein sliding along DNA, this forced hydrated interface (that keeps the protein two layers of water molecules away from the DNA surface) will prevent the protein from sticking to the DNA and allow smoother one-dimensional diffusion.

Oppositely charged surfaces induce interfacial water molecules to adopt an ordered layered structure

We speculate that the formation of an interface between two oppositely charged surfaces induces order in the clusters of solvent molecules trapped between them, which in turn repel the two surfaces at short ranges (Figure 1). The repulsion between the two oppositely charged surfaces caused by the tight binding of water at the interface made the simulation of the transition to a dry interface quite challenging for most of the systems.

To further investigate the layered organization of water near the surfaces, we equilibrated the systems when the two plates were held 10 Å apart. We analyzed the structure of water molecules trapped in-between the two plates in the simulations and found that the ordered arrangement of water molecules is more prominent when the surface charge densities are higher. Water occupancy measurements (Figure 3(a)) show that when the charge density of the negatively charged surface remains unchanged ($\sigma^- = -3$ e nm^{-2}) and that of the positively charged surface increases, the water molecules adopt an increasingly organized arrangement, and an additional layer of water forms upon increasing σ^+ from +2 to +3 e nm^{-2}. As σ^+ increases from 1 to 3, the number of layers of interfacial water increases from 2 to 3.

In addition to the formation of layers of water close to the surfaces, we analyzed the orientation of the water molecules relative to the surface by measuring the orientation angle θ (Figure 3(b)) between the vectors of the dipole moment of the water and the Y axis (vertical to the surfaces, see Figure 1). The cos(θ) value is closer to unity (and therefore the dipole moment of the water molecule is closer to alignment with that of the surfaces) at the same distances at which each an ordered water layer is formed.

The ordering of the water molecules occurs next to both the positively and negatively charged surfaces (Figure 3). However, the orientation angle and the density of water next to the two surfaces are not identical. Based on normalized density calculations, Figure 4 (left column of figures) shows the ordered arrangement of water next to a positively charged surface with σ^+ ranging between 1 and 10 and located 3 nm from the negatively charged surface. The figure clearly shows that the number of water layers, as indicated by the number of peaks in the normalized density curves, increases from 2 to 4 as σ^+ increases. The layers of water are also shifted closer toward the positively charged surface, suggesting tighter binding of the water to the surface. The greater degree of organization of the water at higher charge densities is illustrated in the snapshot shown in Figure 5. Furthermore, the peaks in the density of the water molecules become much sharper and higher as σ^+ increases, providing a molecular explanation for the higher free energy barriers of association of highly charged surfaces. Similar properties of water organization can be seen in the change of the orientation angle, θ, as a function of the distance from the plate (Figure 4, right column of curves). The value of cos(θ) fluctuates and takes higher values at distances that correspond to water layers. Thus, the value of cos(θ) in the first water layer (distance < 0.3 nm from the surface) changes from 0.4 to ~1 upon increasing σ^+ from 1 to 10 e nm^{-2}.

Effect of salt on water organization next to the charged surfaces

We sought to investigate the effect of salt on the organization of water near charged surfaces. Figure 4 shows the density and orientation of water molecules at the interface between two oppositely charged plates for $|\sigma| = 1$, 3, 5, and 10 e nm^{-2} in the presence of NaCl, KCl, or $MgCl_2$

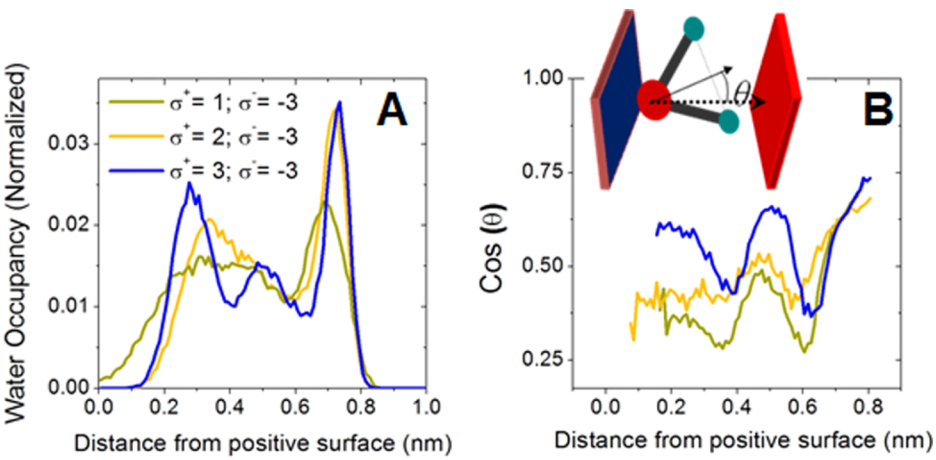

FIG. 3. Organization of water molecules next to surfaces placed 10 Å apart. (a) Density of interfacial water between oppositely charged plates (blue, positively charged; red, negatively charged) in which $\sigma^- = -3$ and σ^+ ranges from 1 to 3. The peaks on the left side correspond to water next to the positively charged surface while those on the right side are related to water next to the negatively charged surface. (b) The orientation angle, θ, of the interfacial water molecules between the vectors of the dipole moment of the water and the Y axis.

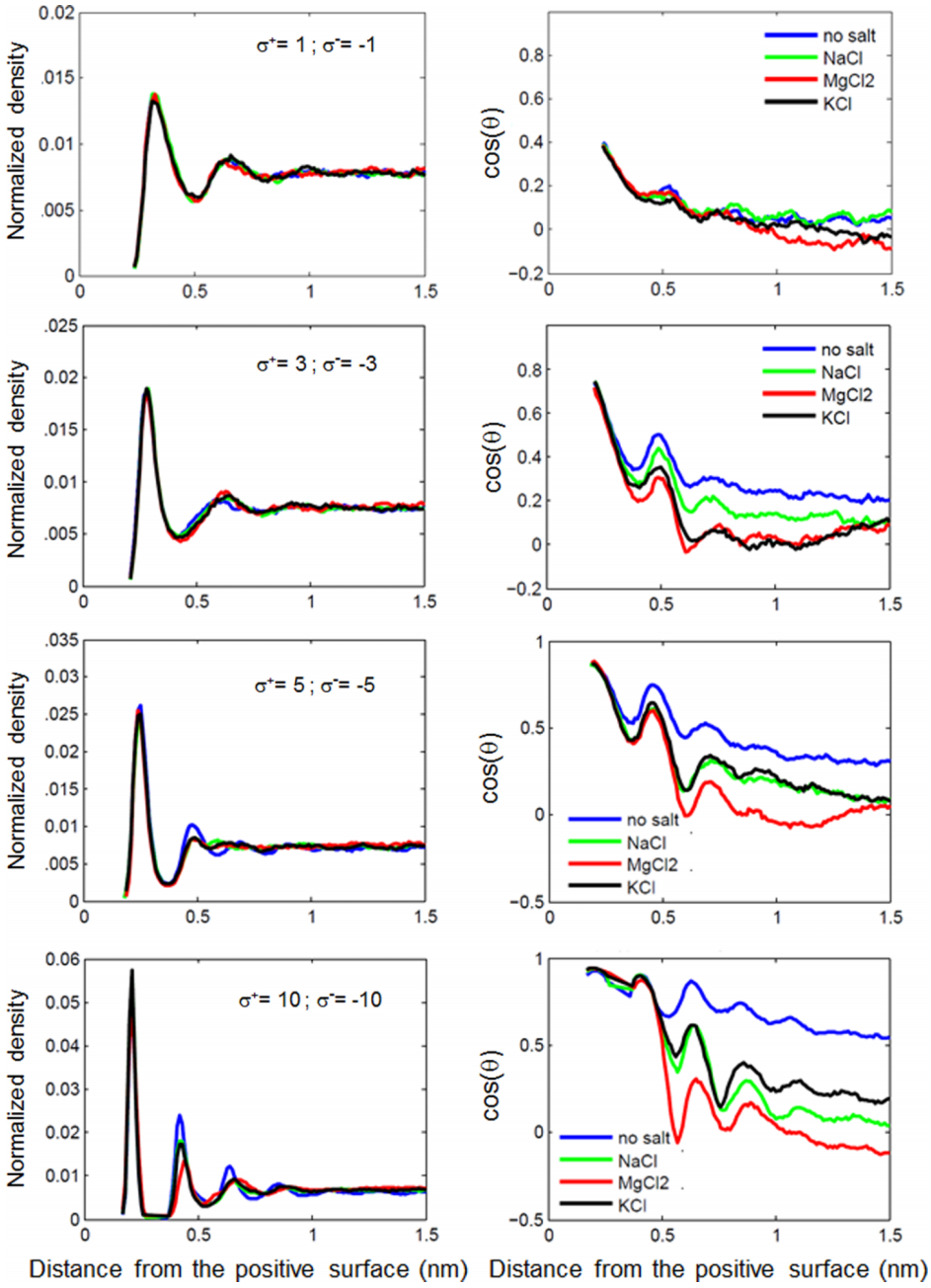

FIG. 4. The effect of salt on the organization of water trapped between two oppositely charged surfaces (blue, positively charged; red, negatively charged) with a charge density magnitude of $|\sigma| = 1–10$ e nm^{-2}. The layering of water is reflected by its normalized density (left) and by the orientation angle adopted by the water molecules (right). Only events occurring at the positively charged surface are shown.

at a concentration of 0.5 M. The addition of salt affects the arrangement adopted by the water molecules at $\sigma^+ = 10$ e nm^{-2}, but lower charge densities scarcely affect the ordering of the water layers. A much stronger salt effect is observed on the orientation angle of the water molecules and is observable even at low and medium surface charge densities, with the effect of divalent ions larger than that of monovalent ions. A similar effect of disruption of the water orientation within the layers was also observed for water next to the negatively charged surface (data not shown), but the effect is stronger adjacent to the negatively charged surface than adjacent to the positively charged surface. This might be explained by cations, such as Na^+ and K^+, having a stronger tendency to adsorb onto a negatively charged surface than Cl^- has to adsorb onto a positively charged surface. The observation that the organization of water next to the surfaces is disrupted by the ions may explain the smoother PMF between two oppositely charged surfaces, and the lower barriers are lower in the presence of salt.

Effect of the size of the surface beads on water organization

The simulated interactions between oppositely charged surfaces showed that charge density dominates the strength of water–surface interactions. For surfaces with a high charge density, the water layers are shifted toward the surface (Figure 4). Figure 5 clearly shows how the water molecules fit the space between the surface beads, particularly for surfaces with $\sigma^+ = 10$ e nm^{-2}.

After observing this geometrical fit between the surface beads and the water molecules, we turned to examine how

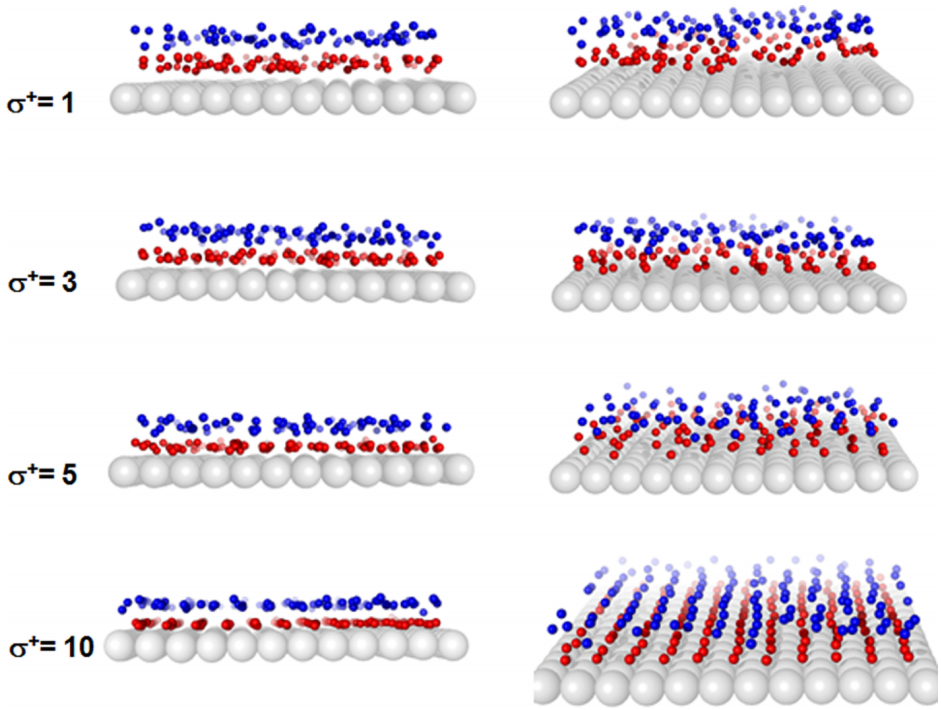

FIG. 5. Snapshots of the first two hydration layers next to the positively charged surface. The first and second layers of water are defined by a distance criterion from the surface. Two orientations of the surface are shown to highlight the increased ordering as σ^+ increases from 1 to 10.

changing the size of the surface beads may affect the organization of water molecules on surfaces with varying charge densities. Figure 6 summarizes the charge density and orientation angle of water molecules next to surfaces bearing different charge densities and comprised of different bead sizes. For larger beads, the water layer forms closer to the surface. Examining the snapshots in Figure 6 suggests that this is because the larger beads create larger pockets on the surface and so enable the surface to accommodate more water molecules. The layers of water are therefore less homogenous as the water can be placed at various sites. This phenomenon is reflected in the lower peaks in the density of water curves (Figure 6). Despite the lower density of water next to plates composed of larger beads, the orientation of the water molecules in these cases is very highly ordered.

Figure 7 shows the location of the water molecules of the first hydration layer on the positively charged surface. For the surface comprised of beads with a diameter of 3 Å, each water molecule is symmetrically placed in-between four surface beads. Surfaces that are composed of smaller 2 Å beads cannot accommodate the water molecules at similar sites, and the hydration layer therefore has a different symmetry. In contrast, a surface with larger beads of 4 Å exhibits a higher water density and the water can be accommodated at various sites. Plotting the hydrogen bonds between the water molecules suggests that the location of the water in the hydration shell is not only determined solely by the surface characteristics (voids, electrostatic forces) but also by the network of hydrogen bonds between the water molecules. The network of hydrogen bonds is not perfect on any of the surfaces, yet it may also govern, at least partially, the water sites on the surfaces. There are water molecules that are involved in 1–3 hydrogen bonds with neighboring water molecules but others that do not form hydrogen bonds with any neighboring water molecule. Figure 7 suggests the existence of frustration between the strengths of water–surface versus water–water interactions. The degree of frustration might be modulated by the surface charge density and the geometry of the surface. These factors may control the location of water sites on the surface and the orientation of the water molecules, and thus influence the ability of the water molecules to form a two-dimensional network of hydrogen bonds.

Implications for non-specific protein–DNA interactions

A major motivation for studying the association between two oppositely charged plates is to estimate the role water has in non-specific protein–DNA interactions, which are assumed to be governed by electrostatic interactions. The simple representation of the flat charged surfaces eliminates the geometrical complexity that may make the simulations, their analysis, and their interpretation more challenging. Although our study included surfaces with the charge density of B-DNA (~1 e nm^{-2}), we performed additional simulations in which the interactions of Na^+ with negatively charged surfaces were studied to verify the value of σ^- of the surface that mimic a B-DNA model.[36,37] Figure 8 shows the density of sodium ions next to a central bead of the negatively charged surface with $\sigma^- = (-1) - (-4)$ e nm^{-2} and next to a B-DNA phosphate molecule. Comparing the condensation of sodium ions on B-DNA with that on the negatively charged surface indicates that the density of Na^+ next to B-DNA is most similar to its density next to the surface with $\sigma^- = -3$ e nm^{-2}. Further support that a charge density of -3 e nm^{-2} for the surface more realistically represents a double-stranded DNA molecule can be obtained by estimating λ (the ratio between the total partial atomic charges in the

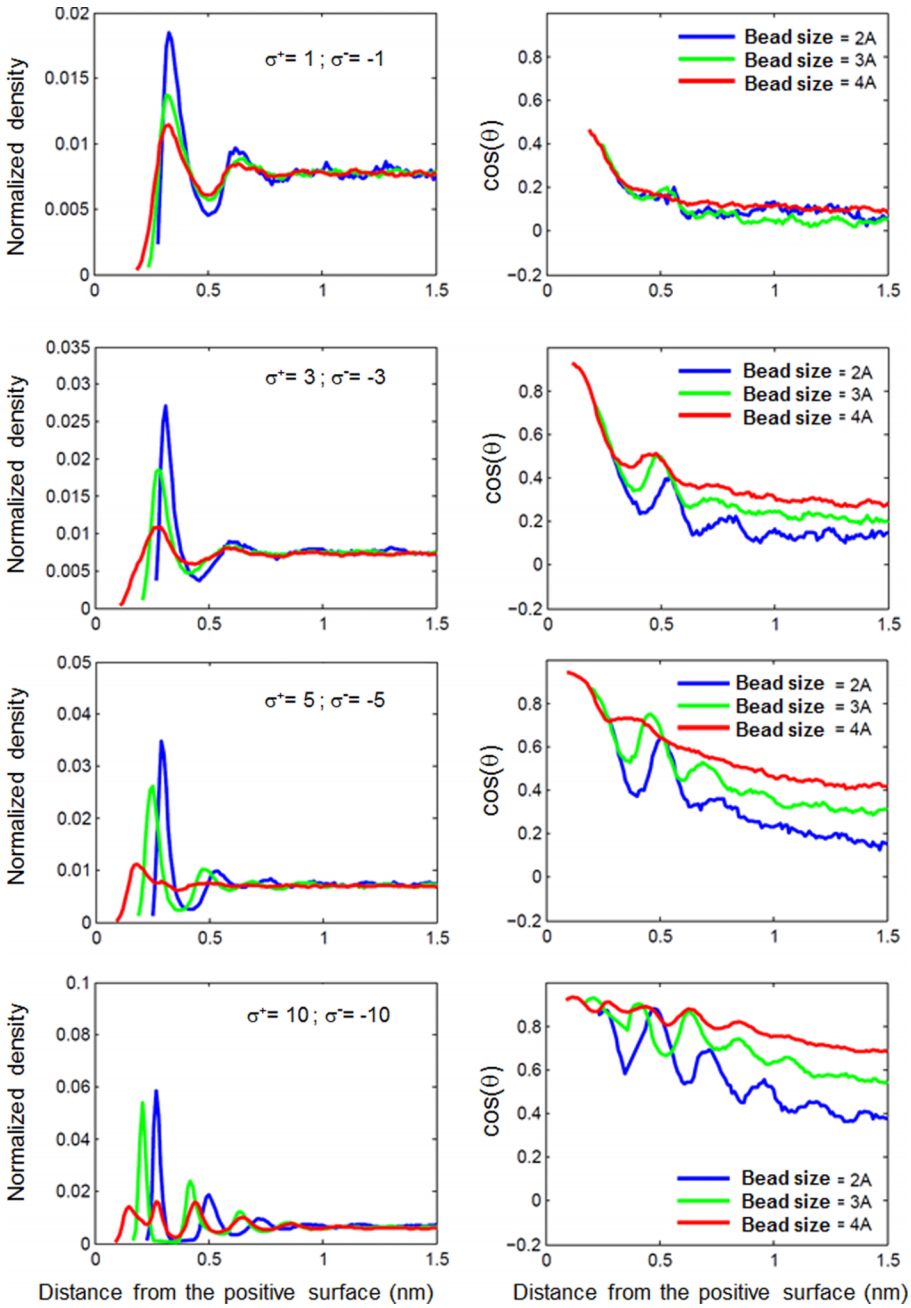

FIG. 6. The effect of bead size on the organization of water molecules trapped between two oppositely charged surfaces with absolute charge densities of $|\sigma| = 1$–10 e nm^{-2}. Three types of surfaces (composed of 6×6 beads) were studied with bead diameters of 2, 3, and 4 Å. The layering of water is reflected by its normalized density (left) and the orientation angle of the water molecules (right). Only the water layers adjacent to the positively charged surface are shown.

system and the solvent accessible area) through calculating the solvent accessible area of the surface or of B-DNA. A λ value of ∼− 0.5 e nm^{-2} is obtained for B-DNA and for a surface that was originally designed with $\sigma^- = -3$ e nm^{-2}. The three times higher charge density of B-DNA double-helix than cylindrical B-DNA can be obtained by a qualitative estimation. As the phosphate charges are localized within the minor grove and because the minor groove is about a third of the total surface of the B-DNA cylinder, the effective surface charge density of the minor groove is expected to be three times higher than the average charge density of the B-DNA cylinder, hence to be −3 e nm^{-2}. Surfaces with $\sigma^- = -3$ have two major hydration layers at which the water molecules exhibit a fairly high degree of alignment with the dipole moment of the surfaces. The PMF for bringing the two surfaces into contact with each other includes two dominant energetic barriers. The barrier that must be crossed to achieve complete dehydration is very high, which suggests that at least a single hydration layer remains between the two planar surfaces. This finding is consistent with the atomistic MD simulations that reported the existence of about two hydration layers at the interface of the complex formed between the SRY protein and DNA.[38,39]

We point out that the charge density of DNA-binding proteins and DNA is often not identical, and σ^+ of the protein is about 4-5 times smaller than σ^- of the DNA.[28] The association of two oppositely charged plates with asymmetric charge density was not investigated in this study but are expected to show a similar pattern of organization of the hydration water while the kinetics being lower as the difference in the charge density increases because of higher free energy barriers for association.

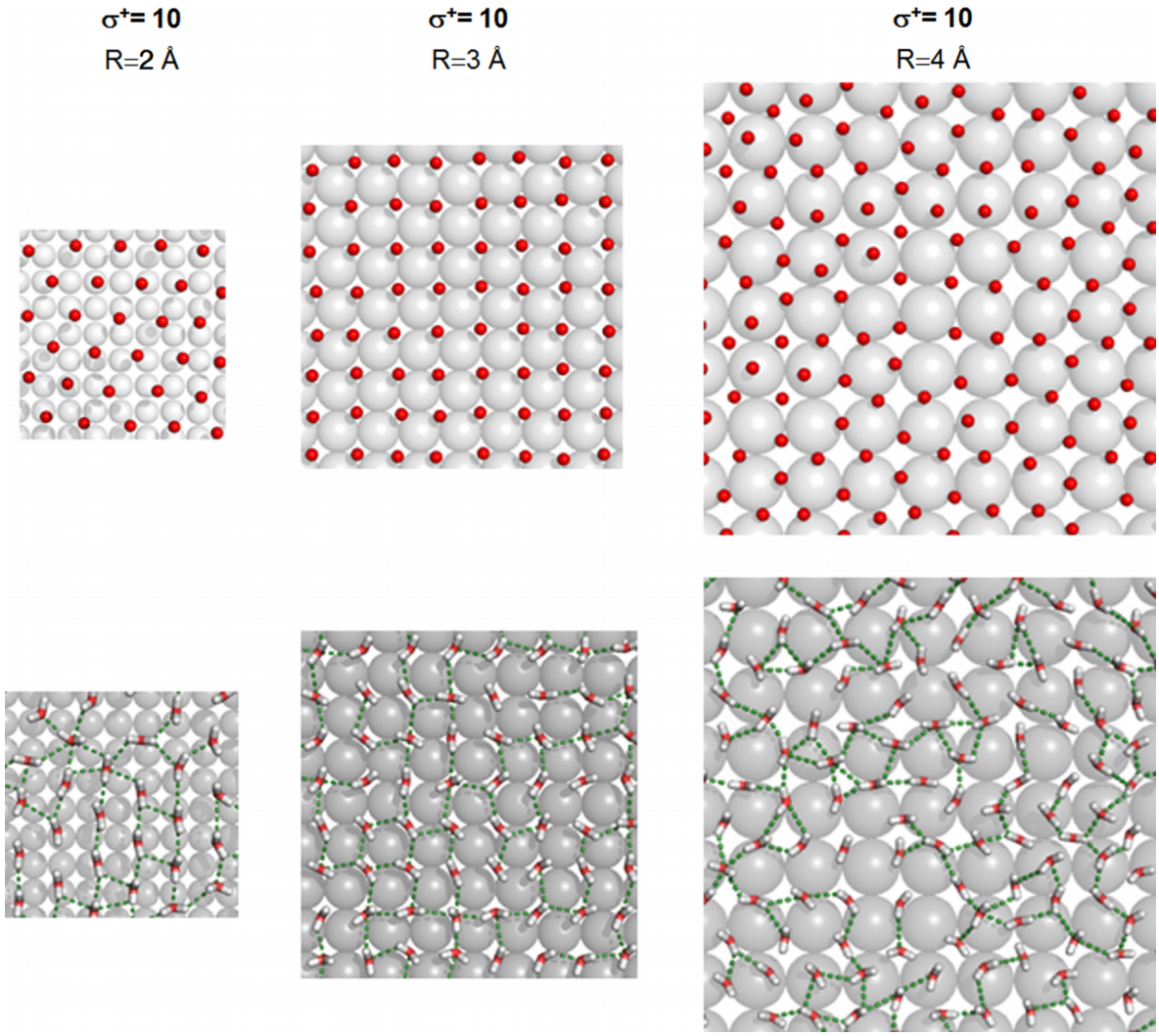

FIG. 7. Snapshots of the first hydration layer next to positively charged surfaces ($\sigma^+ = 10$) comprised of beads of varying size. The upper and lower panels show the location of the water oxygen (in red) and the network of hydrogen bonds formed between the water molecules (green), respectively. The snapshots were taken from a simulation involving a plate composed of 12×12 beads. The size of each panel corresponds to the relative dimensions of the surfaces.

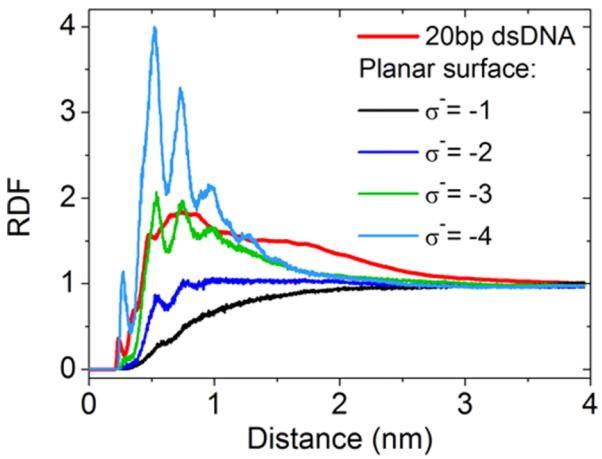

FIG. 8. Interactions between Na^+ and negatively charged molecules. Using the radial distribution function (RDF), the density of sodium ions next to a negatively charged planar surface with σ^- between (−1) and (−4) is compared with the condensation of sodium on a 20 base-pair B-DNA molecule.

CONCLUSIONS

Here, we proposed a model consisting of two charged surfaces immersed in water with and without salt to study the atomistic details of the mechanism by which water may facilitate sliding along DNA. We studied several pairs of surfaces with varying surface charge densities (−σ, +σ) with σ within the range of the macromolecular surface charge densities of DNA and of DNA binding sites on protein surfaces. A calculation of the potential of mean force to bring the two parallel plates into close proximity yields free energy landscapes with a large energetic barrier at short range and additional smaller barriers of 1–2 kcal mol^{-1} along the pathway. This observation strongly depends on the surface charge densities of the two interacting molecules and may indicate that some interfacial solvent molecules and perhaps ions that interact with both surfaces are trapped, with their removal imposing an entropic bottleneck to further approach.

Evidently, nonspecific protein–DNA interfaces tend to be more hydrated compared with the specific binding interfaces,[12,14] where the water molecules are involved in

hydrogen-bonding between the protein side chains and DNA bases.[9] Our study shows that the nonspecific electrostatic attraction between the positively charged protein surface and the negatively charged DNA backbone imposes an ordered layered structure on interfacial water that may repel the positive molecule from the negative molecule. We investigated the organization of the solvent in-between the two plates and found that water molecules assume a layered organization and specific alignment that impose barriers to their removal from the interface. We demonstrated how those trends in the organization of solvent clusters are modulated by the addition of salt, the charge on the surfaces, and by the separation distance between the plates. While our model system demonstrates how salt affects water polarization and layering, it has several limitations (small number of ions and strong repulsive forces) in addressing salt effects at short separation distances where counterions concentration is locally increased and osmotic forces are becoming an important factor.[28] Salt is obviously expected to have a larger effect for the asymmetric case, where positive counterions are strongly concentrated between both plates at short separation, and osmotic forces are becoming an important factor.

We believe that the basic physical-chemical principles studied here explain the commonly observed existence of water in protein–DNA interfaces during specific binding.[14] The presence of 1–2 layers of water within the interface during sliding may screen attractive electrostatic interactions between the positively charged molecular surface on the protein and the negatively charged DNA backbone, and this screening may then reduce intermolecular friction in a manner that maintains a moderate and fairly smooth energetic landscape for sliding and facilitates the 1D diffusion of the protein[19,40] (Figure 9). The reduced ruggedness by the hydration is accompanied by a free energy barrier for dehydration upon localization at the target site and formation of higher affinity interactions (i.e., specific complex).[28] We expect that the magnitude of these effects will strongly depend on the electrostatic properties (e.g., the exact charge density and the degree of homogeneity of the electrostatic surface) and the shape complementarity of the particular protein that approaches DNA for sliding.

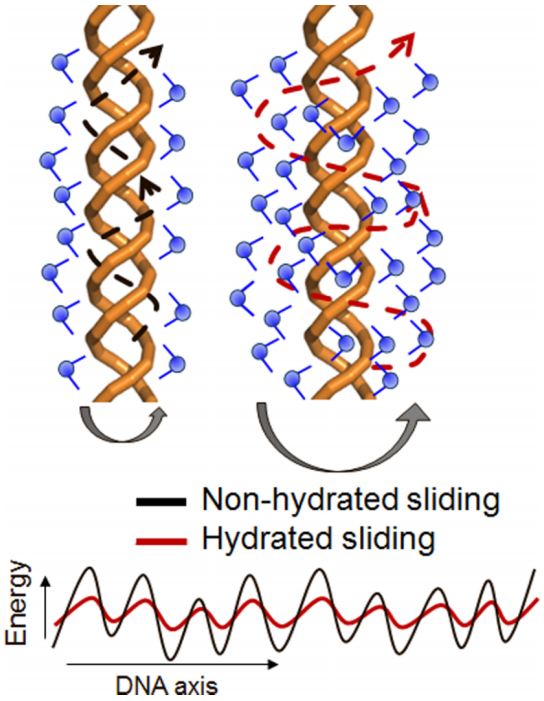

FIG. 9. Sliding of a protein along a DNA molecule. Hydration of nonspecific interfaces in protein–DNA complexes may increase the distance of the protein from the DNA during rotation-coupled translation dynamics (i.e., sliding) and so reduce the energetic roughness of the sliding landscape. Accordingly, the hydration affects the normal energy profile (illustrated, for example, in Fig. 2) and consequently the longitudinal energy profile along the DNA axis. The reduced energetic roughness by the hydration layers is due to weaker electrostatic interactions as well as lower probability for hydrogen bond formation with nonspecific sites.

ACKNOWLEDGMENTS

This work was supported by the Kimmelman Center for Macromolecular Assemblies by the Grant No. 2010424 from the United States—Israel Binational Science Foundation and the Minerva Foundation with funding from the Federal German Ministry for Education and Research. Y.L. is The Morton and Gladys Pickman professional chair in Structural Biology.

[1]Y. Levy and J. N. Onuchic, Annu. Rev. Biophys. Biomol. Struct. **35**, 389–415 (2006).
[2]G. A. Papoian, J. Ulander, and P. G. Wolynes, J. Am. Chem. Soc. **125**, 9170–9178 (2003).
[3]Y. Levy and J. N. Onuchic, Proc. Natl. Acad. Sci. U. S. A. **101**(10), 3325–3326 (2004).
[4]P. Ball, Chem. Rev. **108**(1), 74–108 (2008).
[5]M. Levitt and B. H. Park, Structure **1**(4), 223–226 (1993).
[6]M. Kochoyan and J. L. Leroy, Curr. Opin. Struct. Biol. **5**(3), 329–333 (1995).
[7]A. Savelyev and G. A. Papoian, J. Am. Chem. Soc. **129**(19), 6060 (2007).
[8]C. Materese, A. Savelyev, and G. A. Papoian, J. Am. Chem. Soc. **131**, 15005–15013 (2009).
[9]C. W. Garvie and C. Wolberger, Mol. Cell **8**(5), 937–946 (2001).
[10]J. Janin, Structure **7**(12), R277–R279 (1999).
[11]S. Li and P. Bradley, Proteins: Struct., Funct., Bioinf. **81**(8), 1318–1329 (2013).
[12]M. M. Garner and D. C. Rau, EMBO J. **14**(6), 1257–1263 (1995).
[13]B. Jayaram and T. Jain, Annu. Rev. Biophys. Biomol. Struct. **33**, 343–361 (2004).
[14]T. Lundback and T. Hard, Proc. Natl. Acad. Sci. U. S. A. **93**(10), 4754–4759 (1996).
[15]N. M. Luscombe and J. M. Thornton, J. Mol. Biol. **320**(5), 991–1009 (2002).
[16]M. T. Record, Jr., C. F. Anderson, P. Mills, M. Mossing, and J. H. Roe, Adv. Biophys. **20**, 109–135 (1985).
[17]N. D. Arbuckle and B. Luisi, Nat. Struct. Biol. **2**(5), 341–346 (1995).
[18]C. Chen and B. M. Pettitt, Biophys. J. **101**(5), 1139–1147 (2011).
[19]P. Blainey, G. Luo, S. Kou, W. Mangel, G. Verdine, B. Bagchi, and X. S. Xie, Nat. Struct. Mol. Biol. **16**, 1224–1229 (2009).
[20]M. Slutsky and L. A. Mirny, Biophys. J. **87**(6), 4021–4035 (2004).
[21]O. Givaty and Y. Levy, J. Mol. Biol. **385**, 1087–1097 (2009).
[22]A. Marcovitz and Y. Levy, Proc. Natl. Acad. Sci. U. S. A. **108**, 17957–17962 (2011).
[23]A. Marcovitz and Y. Levy, J. Phys. Chem. B **117**(42), 13005–13014 (2013).
[24]D. Vuzman, A. Azia, and Y. Levy, J. Mol. Biol. **396**(3), 674–684 (2010).
[25]D. Vuzman and Y. Levy, Proc. Natl. Acad. Sci. U. S. A. **107**, 21004–21009 (2010).
[26]L. Zandarashvili, D. Vuzman, A. Esadze, Y. Takayama, D. Sahu, Y. Levy, and J. Iwahara, Proc. Natl. Acad. Sci. U. S. A. **109**(26), E1724–E1732 (2012).
[27]N. Khazanov, A. Marcovitz, and Y. Levy, Biochemistry **52**(32), 5335–5344 (2013).
[28]V. Dahirel, F. Paillusson, M. Jardat, M. Barbi, and J. M. Victor, Phys. Rev. Lett. **102**(22), 228101 (2009).

[29]V. A. Parsegian and D. Gingell, Biophys. J. **12**(9), 1192–1204 (1972).
[30]N. Kampf, D. Ben-Yaakov, D. Andelman, S. A. Safran, and J. Klein, Phys. Rev. Lett. **103**(11), 118304 (2009).
[31]V. Dahirel, M. Jardat, J. F. Dufreche, and P. Turq, Phys. Chem. Chem. Phys. **10**(33), 5147–5155 (2008).
[32]J. L. England, V. S. Pande, and G. Haran, J. Am. Chem. Soc. **130**(36), 11854–11855 (2008).
[33]D. Van Der Spoel, E. Lindahl, B. Hess, G. Groenhof, A. E. Mark, and H. J. Berendsen, J. Comput. Chem. **26**(16), 1701–1718 (2005).
[34]E. J. Sorin and V. S. Pande, Biophys. J. **88**(4), 2472–2493 (2005).
[35]D. Bouzida, S. Kumar, and R. H. Swendsen, Phys. Rev. A **45**(12), 8894–8901 (1992).
[36]A. Savelyev and G. A. Papoian, J. Am. Chem. Soc. **128**(45), 14506–14518 (2006).
[37]A. Savelyev and G. A. Papoian, Proc. Natl. Acad. Sci. U. S. A. **107**(47), 20340–20345 (2010).
[38]B. Bouvier and R. Lavery, J. Am. Chem. Soc. **131**(29), 9864–9865 (2009).
[39]B. Bouvier, K. Zakrzewska, and R. Lavery, Angew. Chem., Int. Ed. Engl. **45**, 196–205 (2012).
[40]R. Zwanzig, Proc. Natl. Acad. Sci. U. S. A. **85**(7), 2029–2030 (1988).